Engineering 4 (2018) 714–721

Contents lists available at ScienceDirect

Engineering

journal homepage: www.elsevier.com/locate/eng

Research
Green Industrial Processes—Article

Intensification of Ethylene Production from Naphtha via a Redox Oxy-Cracking Scheme: Process Simulations and Analysis

Vasudev Pralhad Haribal [a], Yun Chen [a,b], Luke Neal [a], Fanxing Li [a,*]

[a] Department of Chemical and Biomolecular Engineering, North Carolina State University, Raleigh, NC 27695-7905, USA
[b] School of Chemistry and Chemical Engineering, South China University of Technology, Guangzhou 510640, China

ARTICLE INFO

Article history:
Received 12 December 2017
Revised 26 January 2018
Accepted 3 August 2018
Available online 10 August 2018

Keywords:
Ethylene
Naphtha cracking
Process intensification
Chemical looping
Process simulations

ABSTRACT

Ethylene production by the thermal cracking of naphtha is an energy-intensive process (up to 40 GJ heat per tonne ethylene), leading to significant formation of coke and nitrogen oxide (NO_x), along with 1.8–2 kg of carbon dioxide (CO_2) emission per kilogram of ethylene produced. We propose an alternative process for the redox oxy-cracking (ROC) of naphtha. In this two-step process, hydrogen (H_2) from naphtha cracking is selectively combusted by a redox catalyst with its lattice oxygen first. The redox catalyst is subsequently re-oxidized by air and releases heat, which is used to satisfy the heat requirement for the cracking reactions. This intensified process reduces parasitic energy consumption and CO_2 and NO_x emissions. Moreover, the formation of ethylene and propylene can be enhanced due to the selective combustion of H_2. In this study, the ROC process is simulated with ASPEN Plus® based on experimental data from recently developed redox catalysts. Compared with traditional naphtha cracking, the ROC process can provide up to 52% reduction in energy consumption and CO_2 emissions. The upstream section of the process consumes approximately 67% less energy while producing 28% more ethylene and propylene for every kilogram of naphtha feedstock.

1. Introduction

Ethylene is one of the most important organic materials; it is used as a building block to produce fibers, plastics, and other chemicals. Global ethylene production capacity was around 1.48×10^8 t in 2014, representing a 32% increase over the past decade [1]. At present, ethylene is almost exclusively produced via the steam cracking of gaseous and liquid hydrocarbon feedstocks such as ethane, naphtha, and gas oil. Due to its high endothermicity and complex product-separation steps, steam cracking is one of the most energy-intensive processes in the chemical industry. Although ethane is the most common feedstock for cracking in the United States and Middle East, more than 80% of the ethylene produced in Europe and the Asian-Pacific region is from naphtha [2,3].

Naphtha is a mixture of hydrocarbons with a boiling point range of 30–200 °C. In naphtha-based steam-cracking processes, naphtha is first fed into the convective section of the furnace for preheating and vaporization. At elevated temperatures in the radiant section of the furnace (750–900 °C or higher), naphtha is cracked into smaller molecules in the absence of catalysts. Gaseous light olefins are formed via reactions involving free radicals [4,5]. Steam cracking is highly endothermic and requires significant external heat input. Coke deposition, which is inevitable in the complex cracking reaction scheme, represents another significant challenge. Diluting the feedstock with steam lowers the propensity for coke formation. However, cracking furnaces still need to be periodically shut down and regenerated with air to avoid the accumulation of coke. The parasitic energy consumption due to steam usage and the need for periodic shutdowns result in an increase in capital and operating costs [6,7]. From an energy consumption standpoint, the pyrolysis section accounts for approximately 2/3 of the total process energy required in naphtha steam crackers, and leads to about 3/4 of the total exergy destruction [3]. Furthermore, large amounts of carbon dioxide (CO_2) are generated in this process due to the need to combust carbonaceous fuels to satisfy the parasitic energy requirements. Therefore, novel technologies that address these shortcomings of steam cracking are highly desirable.

The oxidative cracking of naphtha using a heterogeneous catalyst is a promising option [8–10]. However, the high reactivity of

* Corresponding author.
E-mail address: fli5@ncsu.edu (F. Li).

https://doi.org/10.1016/j.eng.2018.08.001

the olefins poses a challenge in identifying a suitable catalyst with high selectivity [11]. Moreover, there is an additional difficulty of separating the oxygenate byproducts [6]. The flammability of the gaseous mixture, which contains oxygen (O_2) and fuels, also presents safety concerns. Hot spots can result from over-oxidation of the hydrocarbons to carbon monoxide (CO) and CO_2, lowering the product selectivity [3,12,13]. The current study investigates a two-step, redox oxy-cracking (ROC) process for naphtha conversion in an O_2-free environment. The first step involves selective oxidation of the hydrogen (H_2) produced from hexane cracking with active lattice oxygen in a mixed-oxide redox catalyst. The redox catalyst particles, which enter the reactor at high temperatures, provide the sensible heat to compensate for the endothermicity of the cracking reactions. Meanwhile, the catalyst is reduced during this step. The reduced redox catalyst is later oxidized, regenerated, and reheated in air to complete the redox loop. The absence of gas-phase oxygen in the naphtha conversion step has the potential to ① inhibit the non-selective reaction pathways, ② reduce the potential safety hazards [13–15], and ③ decrease parasitic energy losses by eliminating the air-separation unit and providing tighter temperature control [16]. The overall process also significantly decreases the energy consumption and, hence, the nitrogen oxide (NO_x) and CO_2 emissions. Despite its advantages over steam cracking and conventional oxy-cracking, this novel ROC approach has yet to be investigated in detail.

We recently reported a chemical looping-oxidative dehydrogenation approach for ethylene production from ethane using operational principles similar to those of ROC [17,18]. The redox catalyst development, performance, reaction mechanism, and overall process efficiency were investigated [17–19]. However, these studies were limited to ethane conversion. The oxidative cracking of *n*-hexane to olefins using lattice oxygen of VO_x/Ce-Al_2O_3 has been investigated, showing up to 60% olefin selectivity at 30% *n*-hexane conversion [11]. The performance of sol-gel-synthesized Li/MgO in the oxidative cracking of hexane in the presence of gaseous oxygen, with 28% hexane conversion and 60% selectivity to light olefins, has also been shown [8]. The same authors also studied an integrated plasma-Li/MgO system to improve the oxidative conversion of hexane at the relatively low temperature of 500 °C [9]. Although the integration of plasma was effective to reduce the operating temperature, the light olefin yield was still limited to about 35%. Overall, existing oxy-cracking processes have demonstrated relatively low olefin yields (< 35%). Moreover, studies on the oxy-cracking of naphtha via the chemical looping scheme are limited.

In the current study, a detailed process simulation and analysis is conducted to investigate the performance of the ROC process. Experimental data obtained from a novel redox catalyst composed of alkali-doped mixed oxides were used in the simulation [20]. Single-pass hexane conversions of 79% with 61% light olefin selectivity were achieved in a laboratory-scale reactor. The experimental results were used in the process simulation, and the performance of the ROC process was compared with a state-of-the-art naphtha steam-cracking process. Using ASPEN Plus®, the effects of the reactor and process conditions were investigated (The flowsheets of ASPEN Plus® for hexane cracking and ROC process are given in Figs. S1 and S2 in the supplemental file, respectively). The potential advantages of the ROC process were validated using detailed process analyses. When compared with the steam-cracking process, the net energy demand of the upstream section of the ROC reference case (79% naphtha conversion) was shown to be 67% lower, and to require 25% less compression work. These decreases result in a 52% drop in the overall energy demand and a corresponding reduction in CO_2 emissions, as compared with the conventional cracking process.

2. Process descriptions

Naphtha can vary in composition depending on its source and refinery conditions. It is a complex mixture of hydrocarbons that ranges from straight-chain alkanes to aromatics. One of the major components of naphtha is *n*-hexane. Reaction (1) illustrates one of the representative cracking reactions of *n*-hexane to ethylene. In addition to its high endothermicity, the vaporization of naphtha can be energy consuming—the enthalpy of vaporization for *n*-hexane at 298 K is 359 $kJ \cdot kg^{-1}$. A simplified process flow diagram for the conventional naphtha steam-cracking process is shown in Fig. 1(a). As the first step, preheated naphtha is thermally cracked in the presence of steam. Since naphtha cracking is equilibrium limited and tends to form coke, steam is used as a diluent to enhance naphtha conversion and inhibit coke formation. In the cracking step, naphtha is passed through the tubes of the cracking furnace. The furnace is operated at high temperatures (~1000 °C), so the heat for the endothermic cracking reactions is provided by the fuel combustion. The furnace consists of the radiant zone, where the cracking reaction occurs at > 750 °C, and the convective zone, where the feedstock preheating takes place at up to 650 °C. The product stream is at a temperature of approximately 800 °C. Using transfer line heat exchangers, the stream is rapidly quenched to 300–400 °C. This avoids further cracking and preserves the product compositions. As the product contains significant amounts of heavy hydrocarbons, a primary fractionator is installed to remove tar and oily material (boiling point > 200 °C) from the cracked gases. The product is further quenched to near-ambient temperature to remove the "heavies." This is followed by a multistage compression system to raise the pressure of the lighter gaseous products to around 4 MPa. Drying and acid gas removal (AGR) units are present at the intermediate compressor stages, as they need to be operated at high pressures. An adsorption column of molecular sieves facilitates the drying, followed by a caustic wash to remove acid gases such as CO_2. The formation of hydrates is prevented by having the drying unit before the caustic wash [2].

$$C_6H_{14}(g) \rightarrow 3C_2H_4 + H_2 \qquad \Delta H_{1048K} = +319.6\ kJ \tag{1}$$

The light components from the compressed stream are sequentially separated from the heavy fractions using a separation train of distillation columns that ultimately yield high-purity ethylene and propylene. At the beginning of the sequence, methane (CH_4) and lighter components (primarily H_2) are selectively separated using a demethanizer (DM). A deethanizer (DE) column separates acetylene, ethane, and ethylene from the bottom product of the DM. The distillate of the DE is reacted with H_2 to convert acetylene to ethylene, and then further distilled using a C2 splitter to generate the ethylene product. The C3+ components exit at the bottom of the DE, and are further purified in a depropanizer (DP) to separate the C4+ components. The debutanizer (DB) separates the C4 materials, raw pyrolysis gasoline, C5 materials, and aromatics from the bottom of the DP [2]. The C3 splitter follows the DP and recovers propylene, which is a valuable product.

Fig. 1(b) depicts the naphtha ROC process. A reactor-regenerator scheme is used instead of the energy-intensive furnaces. An experimental product distribution for the ROC scheme, using an alkali-doped calcium-manganese (Ca-Mn)-based oxide similar to that reported in our previous work [20], is used in the current work. For the ASPEN Plus® simulations, an oxide mixture containing calcium oxide (CaO) and manganese oxide (MnO_x) is used because the specific mixed-oxide is not available in the ASPEN Plus® database. Mn_3O_4 acts as the oxygen carrier phase participating in the oxidative dehydrogenation (ODH) reaction through lattice oxygen donation. Mn_3O_4 is reduced to MnO following Reaction (2). Naphtha is converted to a variety of products; however, for simplicity, Reaction (2) portrays *n*-hexane to ethylene

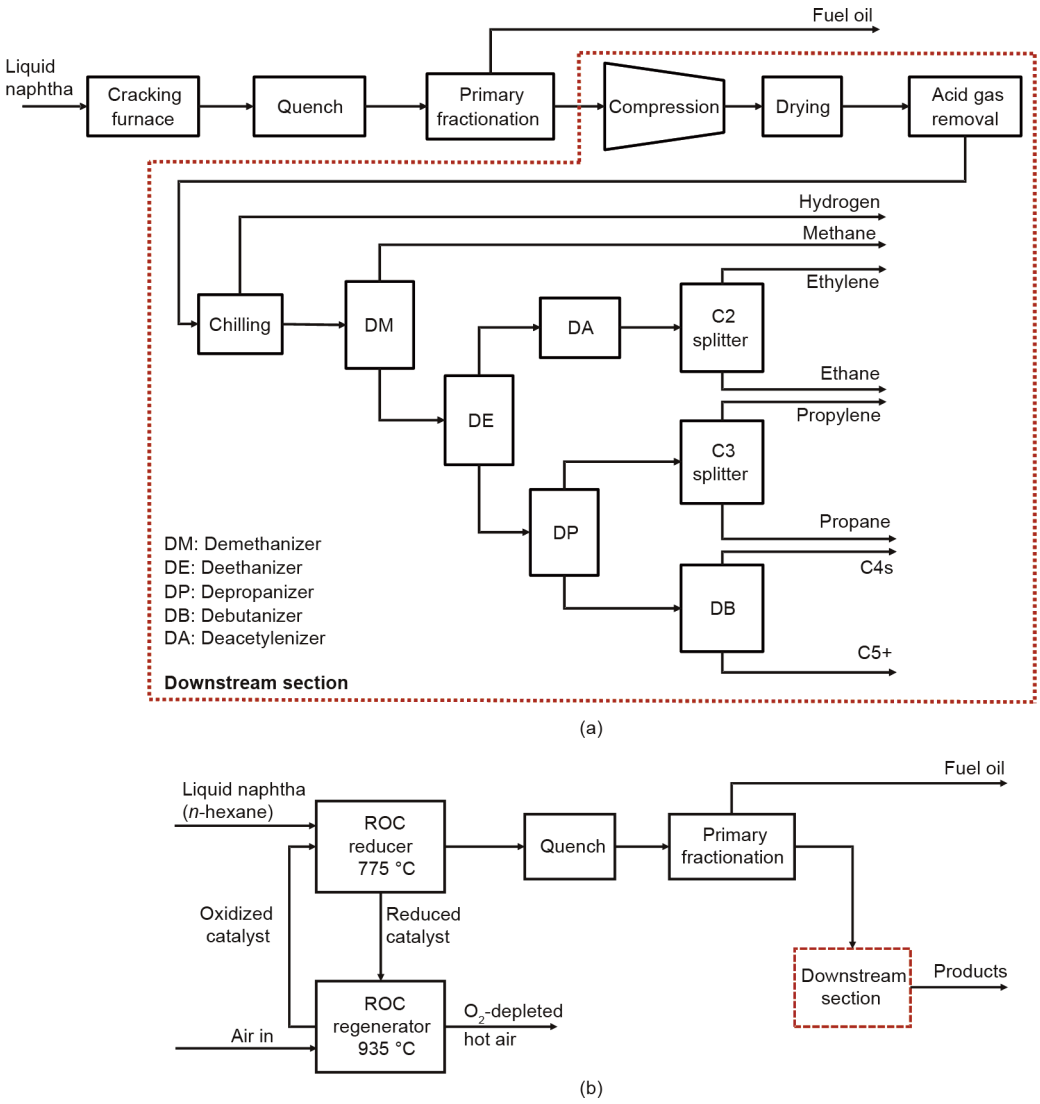

Fig. 1. (a) Simplified process scheme of naphtha steam-cracking process; (b) simplified schematic of the ROC process.

as the model reaction, which involves the combustion of H_2 to water. In a regenerator, the reduced redox catalyst (oxygen carrier) is replenished with air via Reaction (3) (which is highly exothermic). The ASPEN Plus® database values indicate that the surrogate catalyst exhibits similar heat of reaction and heat capacity values to those of the actual redox catalysts. In the current work, the reducer is operated at 775 °C and 1 atm (1 atm = 1.013×10^5 Pa), while the regenerator is operated at 935 °C and 1 atm. The redox loop is completed by recirculating the re-oxidized particles to the reducer. The redox catalyst provides both the necessary lattice oxygen and the heat required for ROC reactions. The naphtha and the air are preheated to 650 °C. The oxygen-depleted hot air from the regenerator is used to generate high-pressure steam to compensate for parasitic energy requirements. The gaseous output from the reducer passes through a series of downstream separation units similar to steam cracking. An amine scrubbing unit for CO_2 removal is required for the ROC process, as this process produces more CO_2 than traditional cracking. The heat requirements of the reducer and naphtha preheating are sufficiently provided by the heat stored in the re-oxidized solids. This is possible due to their high heat capacity and to the temperature difference (ΔT) between the reducer and regenerator. The reducer is endothermic, whereas the regenerator is exothermic. The reducer-regenerator system is operated under adiabatic conditions. The cracking furnace constitutes a major share of the total energy requirement; since it is replaced by the ROC reactors, the energy demand is reduced. In the following sections, the ROC process is compared with naphtha cracking based on the overall energy requirements.

$$C_6H_{14}(l) + Mn_3O_4 \rightarrow 3C_2H_4 + 3MnO + H_2O \quad \Delta H_{298K} = +341.3\ kJ \tag{2}$$

$$3MnO + \frac{1}{2}O_2 \rightarrow Mn_3O_4 \qquad \Delta H_{298K} = -227.8\ kJ \tag{3}$$

3. Simulation assumptions

The performance of ROC was evaluated and compared with naphtha steam cracking using the ASPEN Plus® simulator [21]. Two kinds of naphtha feeds were used to model the cracking process: ① a complex naphtha consisting of a variety of hydrocarbons, based on literature data; and ② *n*-hexane. Since *n*-hexane is a major component of naphtha, the process model can be significantly simplified, provided that the results using the *n*-hexane feed provide a reasonable representation of those using the complex feed. The composition of the complex naphtha is shown in Fig. 2, which has been optimized to mimic "true" naphtha. For the

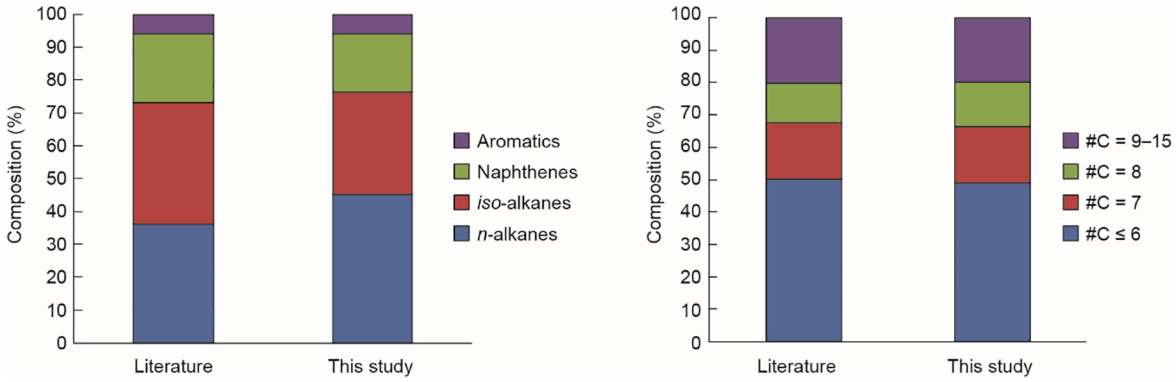

Fig. 2. Composition chosen to represent complex naphtha. (a) Based on Ref. [2]; (b) based on Ref. [22].

simplicity of the model, pure *n*-hexane was used as a representative compound for naphtha in the ROC process. Table 1 summarizes the ASPEN Plus® modules, property methods, and physical property databanks, while Table 2 lists the carbon yields for the various processes. The cracking results are based on literature data [2,22], whereas the ROC results are experimental results that were published in our previous work [20]. A higher hexane conversion case was also considered, in which 97% of the hexane is assumed to be converted in the ROC process. Experiments on blank hexane cracking and the ROC case revealed an increase of roughly 30% in ethylene and propylene yield for the ROC. Keeping the CO_x yield similar to that in the base ROC case, the ethylene and propylene yields were proportionally increased for the high ROC case, with the overall hexane conversion being 97%. The other products were assumed to have yields similar to that of the base ROC. The product distributions of this hypothetical high ROC case are given in Table S1 in the supplemental file. The supplemental file also contains general information with respect to process configuration in ASPEN Plus®, materials flow, etc.

The drying unit and the primary fractionator were modeled as flash columns, in which almost all of the water is condensed along with the heavy hydrocarbons. To simulate the AGR unit, a separator (Sep) was used, with its energy consumption accounted for. This was placed at the exit of the compressor. The solids used in the simulation include Mn_3O_4 and MnO, with CaO added as an inert substance in order to closely represent the actual redox catalyst [20]. Table 3 lists the key operating conditions and simulation assumptions.

In both the complex and *n*-hexane feed cases, the hydrocarbon feedstock is introduced to the cracking furnace after being preheated to 650 °C along with steam. A steam dilution of 0.5 kg per kilogram fresh feed is used [2]. The same preheating temperature

Table 2
Carbon yields for the cases investigated.

Component	Carbon yields (%)		
	Complex feed	*n*-hexane feed	ROC
H_2	0	0	0
Methane	11.5	9.6	7.7
Acetylene	0.7	0.6	0.3
Ethylene	27.3	27.3	32.0
Ethane	3.3	2.8	2.1
Propadiene	0.8	0.7	0
Propylene	12.3	10.3	16.2
Propane	0.3	0.2	0.6
C4s	0.2	0.2	0
Butadiene	4.1	3.4	4.0
Butene	2.8	2.4	7.5
Butane	0.2	0.1	0.1
Benzene	13.3	11.2	0.2
Toluene	2.6	2.2	0
Xylene	1.0	0.9	0
Ethyl benzene	0.4	0.3	1.8
Styrene	1.3	1.1	0
Naphthalene	0	0	0
n-pentane	4.4	1.7	1.5
n-hexane	1.1	18.0	21.4
iso-heptane	3.1	1.7	0
iso-octane	2.5	0.8	0
Cyclohexane	3.2	0.8	0
TMB	1.1	0.9	0
Dodecane	2.5	3.0	0
CO	0	0	1.3
CO_2	0	0	3.4
Naphtha conversion	82[a]	82[b]	79[b]

[a] Equal conversions of all the feed components assumed are listed in Table 1.
[b] Conversion of *n*-hexane.

Table 1
Modules, property methods, and physical property databanks used in ASPEN Plus®.

Process simulation components		Settings in ASPEN Plus®
Stream class		MIXCISLD
Databank		PURE, AQUEOUS, SOLIDS, INORGANIC
Solid components		Mn_3O_4, MnO, CaO
Property method		PR-BM and STEAM–TA for steam cycles
Unit operation modules	Regenerator, reducer, and deacetylenizer	RStoic
	Cracking reactor/furnace	RYield
	Pressure changers	MCompr
	Heat exchangers	Heater
	Distillation columns	DSTWU
	Separators/flash columns	Sep/Flash2

Table 3
Key operating conditions and simulation assumptions.

Process simulation parameters	Settings in ASPEN Plus®
Ambient condition	T = 25 °C, P = 1 atm (1.013 × 10^5 Pa)
Reaction assumptions	As per the carbon yield distribution in Table 3
Chemical looping reactor operating pressure	1 atm
Deacetylenizer operating pressure	25 atm
Compressor specifications	Four stages with intercooler at 25 °C, isentropic efficiency of 0.72
Air feed (to the regenerator)	10% excess
Discharge temperatures to the environment	25 °C
Thermal energy to steam efficiency	85%
Thermal energy to electric energy efficiency	40%

is used in the ROC case, without steam dilution. In the process simulation, the Mn_3O_4-containing redox catalyst particles are initially fed into the reducer. They are reduced and flow to the regenerator, which is maintained at 935 °C, with the temperature of the reducer at 160 °C lower. In the regenerator, 10% excess air preheated to 650 °C is used to completely oxidize the reduced oxygen carrier (Reaction (3)) prior to recirculation to the reducer for another redox loop. Based on the product distribution in Table 2, the ROC involves the combustion of 75% of the H_2 to H_2O.

To prevent further cracking, the product gases in all the cases are quenched to a temperature of 100 °C. Heat released from the quenching is assumed to be utilized to generate steam and preheat the feed streams. The exothermicity of the reactor-regenerator system can also produce low-pressure steam, which can reduce the upstream energy load. The cooled gases are compressed to 2.5 MPa and flashed at 100 °C, in order to remove the heavy hydrocarbons and water from the stream. In the present model, this compressor, with the flash column, functions as the primary fractionator. The light stream is further compressed to a pressure of 42 atm [2] using a four-stage isentropic compressor. The primary component of acid gas is assumed to be CO_2, with no hydrogen sulfide (H_2S) present. Negligible energy consumption is assumed for the caustic wash. For the ROC, which has substantially more CO_2 in the product stream, an amine scrubbing process is assumed, with an energy consumption of 0.11 MW·h per tonne CO_2 [23]. Table 4 lists the operating conditions of the downstream columns for the cracking process [24]. The compressed stream is cooled to −100 °C prior to methane removal in the DM. This refrigeration step reduces the load on the DM by removing most of the H_2 and CO. A single pass is assumed in all the cases. The reflux ratio for each column is fixed as twice that of the minimum reflux ratio. For a fair comparison, the same number of stages and recovery were assumed for the C2 splitters in both cases. A deacetylenizer is used after the DE, in order to hydrogenate the acetylene in the DE distillate (see Table S1 in the supplemental file). Purified H_2 for this reaction is obtained through pressure swing adsorption (PSA), which operates with 80% H_2 recovery, an exit purity of 99% H_2, and a pressure drop of 0.1 MPa [25].

For process comparison, the different forms of energy (thermal, steam, and electricity) are converted into the same thermal basis. The higher heating value efficiencies used for different energy conversions are given in Table 3. The refrigeration power is calculated using the power-temperature graph provided in Ref. [26], and using the condenser and reboiler duties of the columns, as calculated by ASPEN Plus®. Table 4 [24] lists the refrigerants chosen for each unit.

4. Results and discussion

4.1. Effect of feed compositions

Using the product distribution shown in Table 2, both the complex naphtha and the pure *n*-hexane feed were simulated for the conventional steam-cracking process. Fig. 3 shows the similarities in the properties of the two feeds. Typically, a naphtha cracking unit has an overall energy demand in the range of 20–40 GJ per tonne ethylene [3]. Table 5 illustrates the overall and unit-wise energy distribution of the two cases with the complex and *n*-hexane feeds. As can be seen, the results from the pure *n*-hexane feed are very similar to the results from the complex naphtha feed. This indicates that *n*-hexane can be used as a suitable model compound for naphtha, without compromising the accuracy of the simulation results. Fig. 3 breaks down the energy consumption of each section relative to the overall energy demand for both the pure *n*-hexane and the complex feeds. Again, close agreement was obtained.

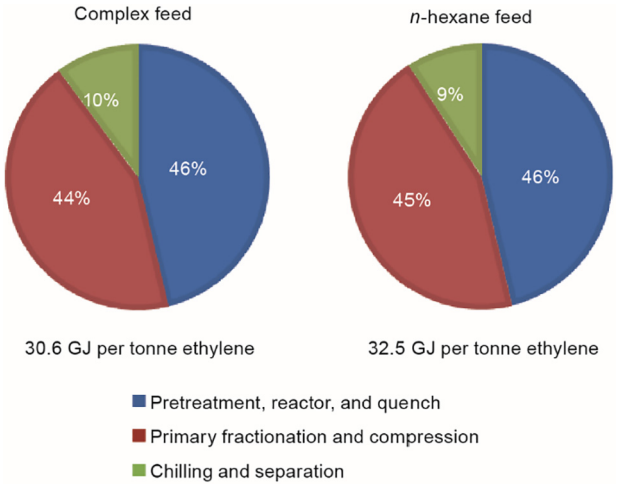

Fig. 3. Section-wise energy distribution for naphtha cracking.

4.2. Energy distributions in steam cracking

Considering the similarities of the results from the complex and *n*-hexane feeds, *n*-hexane was used to represent naphtha in the rest of the studies. The ASPEN Plus® simulation of the naphtha cracking process indicates an energy consumption of 32.5 GJ per tonne ethylene. This finding is in agreement with the study of Ren et al. [3], which reports an energy consumption range of 20–40 GJ per tonne ethylene. For the cracking process, 78% of the total energy is required in the upstream section of the process. Quenching of the hot gases generates high-pressure steam and recovers additional energy. The compression step corresponds to 57% of the overall downstream energy consumption, while the refrigeration for the DM feed and the C2 splitter consumes 17% and 16% of the downstream energy, respectively, with the C2 splitter being the most energy-intensive separation column.

4.3. Process comparisons

As shown in Table 3, the conversions are comparable for the cracking and ROC base cases; however, the ROC process offers a

Table 4
Details of the distillation columns [24].

Unit	Key components (heavy/light)	Recoveries (heavy/light, %)	Reflux ratio	Pressure (MPa)		Temperature required (°C)/refrigerant
				Condenser	Reboiler	
Demethanizer	Ethylene/methane	99.90/0.50	3.0	2.6	2.7	−95/ethylene
Deethanizer	Propane/ethylene	99.99/0.10	0.6	1.0	1.1	−43/ethane
Depropanizer	*iso*-butylene/propylene	99.99/1.40	4.6	1.0	1.1	25/propylene
C2-splitter	Ethane/ethylene	99.00/0.06	2.7	0.4	1.1	−76/ethylene
C3-splitter	Propane/propylene	99.60/0.24	18.0	1.6	1.8	34/propylene
Debutanizer	Butadiene/*iso*-butane	99.90/0.10	8.6	0.4	0.5	32/propylene

Table 5
Overall and unit-wise energy distribution for complex naphtha and *n*-hexane feeds (unit: GJ per tonne ethylene).

Unit	Section	Complex feed	*n*-Hexane feed
Upstream	Reactor (endothermicity)	8.04	8.72
	Feed pretreatment	7.80	8.27
	Steam heat	6.85	7.19
	Quench	−8.53	−9.17
	Primary fractionation	9.68	10.44
Upstream total		23.84	25.44
Downstream	Compressor	3.66	4.03
	Demethanizer	0.40	0.45
	Deethanizer	0	0
	Depropanizer	0.16	0.14
	C2-splitter	1.16	1.13
	C3-splitter	0.49	0.40
	Debutanizer	0.01	0.01
	Deacetylenizer	0.08	0.09
	CO_2 scrubbing	0	0
	PSA	0.03	0.03
	Chilling	0.79	0.74
Downstream total		6.78	7.02
Total		30.6	32.5

Table 6
Comparison of the energy demands (unit: GJ per tonne ethylene).

Unit	Section	*n*-hexane cracking	ROC
Upstream	Reactor (endothermicity)	8.72	0
	Feed pretreatment	8.27	8.56
	Air/steam preheat	7.19	2.98
	Quench	−9.17	−7.93
	Heat released	0	0
	Primary fractionation	10.44	4.70
Upstream total		25.44	8.32
Downstream	Compressor	4.03	3.02
	Demethanizer	0.45	0.38
	Deethanizer	0	0.05
	Depropanizer	0.14	0.16
	C2-splitter	1.13	1.18
	C3-splitter	0.40	0.53
	Debutanizer	0.01	0
	Deacetylenizer	0.09	0.15
	CO_2 scrubbing	0	0.30
	PSA	0.03	0.01
	Chilling	0.74	1.4
Downstream total		7.02	7.17
Total		32.5	15.5

Note: The high-value products (HVPs) yield in *n*-hexane cracking is 2.5 kg per kilogram ethylene; the HVPs yield in ROC is 2.0 kg per kilogram ethylene.

28% increase in the combined ethylene and propylene yield, which are the main products of the process. Fig. 4 shows the section-wise energy distributions of the naphtha cracking process and the ROC case. Table 6 lists the energy distributions for the two processes. The cracking process requires the energy-intensive furnace, which contributes about 27% of the overall energy demand. In the ROC case, the furnace is replaced by the reducer-regenerator system, which is operated based on cyclic redox reactions (Reaction (2) and Reaction (3)). The regenerator replenishes the O_2 in the carrier via the highly exothermic Reaction (3). The nitrogen (N_2)-rich hot air exiting the regenerator is used to generate high-pressure steam, and provides upstream energy in the ROC case. As the reactors are operated adiabatically, the upstream and overall energy requirements for the ROC case are reduced significantly. The absence of dilution steam further reduces the upstream (thermal) energy demand and decreases the upstream demand from 25.44 GJ per tonne ethylene for cracking to 8.32 GJ per tonne ethylene for the ROC case, as shown in Table 6. This upstream section shows the most significant reduction in energy demand in ROC compared with cracking.

The compression section provides the main energy savings downstream in the ROC, with a 25% reduction compared with cracking, due to a decrease in the total moles of the product gases, on a dry basis. The overall downstream energy requirement is roughly the same for the two cases. The refrigeration duty needed to cool the feed to the DM is reduced, as less mass is fed to the DM in the ROC case. Overall, 0.11 MW·h of work per tonne of CO_2 captured is needed for the ROC process [23]. Assuming 100% CO_2 removal, this accounts for 0.12 GJ (electric) per tonne ethylene, contributing roughly 4% of the downstream energy demand. The PSA unit contributes an energy requirement of 2.2 kW·h (electric) per kilogram H_2 separated [25]. The ROC involves the separation of a lesser amount of H_2, leading to reduced PSA energy requirements. In both cases, the deacetylenizer operates at high pressures (~2.5 MPa) and at temperatures of 50–70 °C [27]. The reactant gas from the top of a DE is at a very low temperature (−50 °C). Higher ethylene to ethane and propylene to propane ratios lead to higher C2 and C3 splitter energy demands. Overall, the ROC case has the potential to provide a 52% reduction in the overall energy demand of the plant, compared with *n*-hexane cracking, as shown in Fig. 4. For process analysis purposes, we considered both the ethylene product and the high-value products (HVPs). Here we followed the definition of HVPs by Ren et al. [3], which considered all the olefins and C5+ hydrocarbons including aromatics as value-added products. Figs. 5 and 6 compare the two cases by normalizing the energy demand in terms of the HVPs.

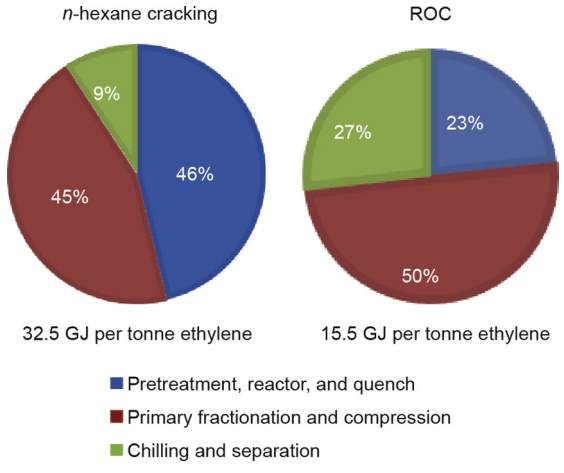

Fig. 4. Section-wise energy distributions of the *n*-hexane cracking and the ROC.

4.4. Net demand and emission comparisons

The cracking and the ROC process produce fuel gases (CO, CH_4, and H_2), which can be combusted to meet the energy requirements. Assuming that all the fuel gases are used, the *n*-hexane cracking shows a deficit of 5.2 GJ per tonne ethylene, which represents 16% of the total demand. In comparison, the ROC process requires no further fuel input, as calculated using the $\Delta H_{reaction}$ in Table 7 and the amount of available fuel based on ASPEN Plus®. In the steam-cracking case, a portion of the fuel oil can also be combusted to meet the energy demands. For simplicity, no fuel oil recycling was considered in this study, although fuel oil can be used as a feedstock to increase the ethylene and propylene yields.

This section compares the two processes based on the net energy required to produce 1 t of ethylene. In this analysis, we used the energy values of the feedstock and products to determine the net energy consumptions for ethylene production. This permits an impartial comparison of the conventional and ROC processes,

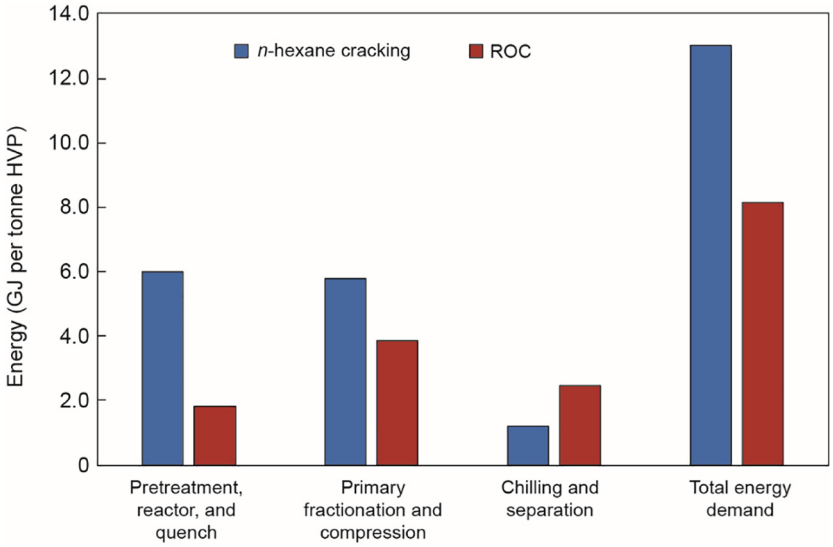

Fig. 5. Comparison of the energy distributions in steam cracking and ROC processes. HVP: high-value product.

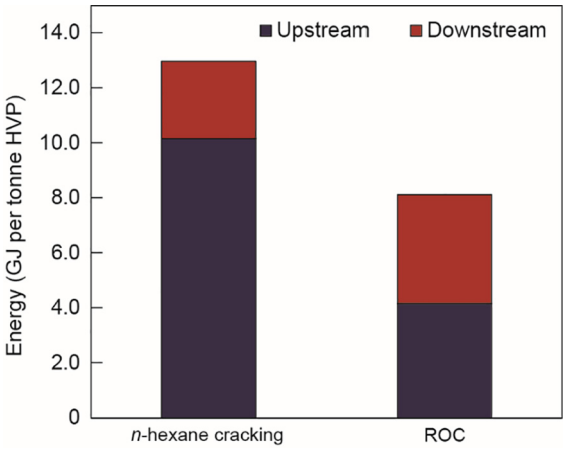

Fig. 6. Normalized energy demand (section-wise and overall) in steam cracking and ROC processes.

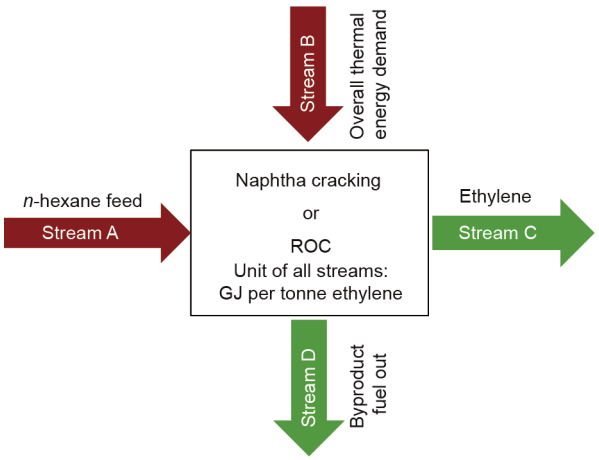

Net energy demand = Stream A + Steam B − Stream D

Fig. 7. Schematic for net energy demand analysis.

Table 7
$\Delta H_{reaction}$ and molar flow rates of the byproduct fuels.

Component input	Heat release (LHV)	
$CO + \frac{1}{2}O_2 \rightarrow CO_2$	282 kJ·mol^{-1}	
$CH_4 + 2O_2 \rightarrow CO_2 + 2H_2O$	800 kJ·mol^{-1}	
$H_2 + \frac{1}{2}O_2 \rightarrow H_2O$	239 kJ·mol^{-1}	
Fuel oil (heavy hydrocarbons)	43.3 MJ·kg^{-1} (Cracking) 45.0 MJ·kg^{-1} (ROC)	
Component output	**Cracking (mol per mole C_2H_4)**	**ODH (mol per mole C_2H_4)**
CO	0	0.085
CH_4	0.718	0.488
H_2	0.804	0.080

since one could argue that ROC's primary energy "savings" result from indirect combustion of H_2 and hydrocarbons. As shown in Fig. 7, the entire process is divided into four relevant energy streams: ① the *n*-hexane feed (stream A); ② the overall thermal energy demand (stream B); ③ ethylene (the main product) (stream C); and ④ the byproduct fuel out (stream D). Lower heating values (LHVs) are used for the fuel streams and are normalized based on 1 t of ethylene produced.

As shown in Fig. 8 below, the ROC process requires 14% less *n*-hexane per tonne of ethylene produced owing to higher ethylene yields, along with being less-energy intensive compared to traditional naphtha cracking. For every tonne of ethylene produced, the ROC process requires a net energy feed of 67 GJ, leading to 39% savings in overall process energy consumptions.

In the case of *n*-hexane cracking, a negligible amount of CO_2 is present in the product gases. Here, it is assumed that methane is used to meet the energy requirements in both the cracking case and ROC. Based on the LHV of CH_4 and the total energy demand of the two processes, as given in Table 7 and Fig. 5, 40.6 and 19.4 kmol CH_4 are required to get 1 t ethylene for the cracking case and for ROC, respectively. This leads to an emission of 1.8 and 0.85 kg CO_2 per kilogram ethylene, respectively. Ren et al. [3] report an emission of 1.8–2 kg CO_2 per kilogram ethylene for naphtha cracking units. Therefore, ROC has the potential to result in a 52% reduction in CO_2 emissions. The ROC process does not need high-temperature furnaces. Therefore, significantly reduced NO_x emissions can also be anticipated [28]. The overall thermal energy demand for the high ROC case is 14 GJ per tonne ethylene, which provides an energy reduction of 10% and 57% compared with the base ROC and cracking cases, respectively, with proportional reduction in CO_2 emissions. As shown in Fig. 8, although the net demand

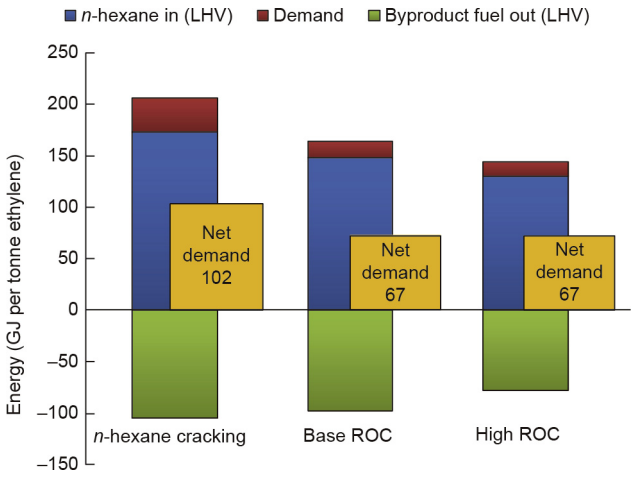

Fig. 8. Net (thermal) energy demand for ethylene production. (The net energy demand shown here follows the definition from Fig. 7 and is defined differently from the energy demand presented in Sections 4.1–4.3)

remains unchanged for the ROC cases, the ROC high conversion case provides a reduction of 12.8% in the *n*-hexane feed and 10% in the overall energy demand for every tonne of ethylene produced.

5. Conclusion

The current study investigates an ROC process for light olefin production from naphtha. Based on our recently obtained experimental data using an Mn-based redox catalyst, the ROC process was simulated using ASPEN Plus® and compared with the traditional steam-cracking process. Compared with cracking, ROC replaces the energy-intensive cracking furnaces with an autothermal reducer-regenerator system. This results in significant energy savings. Moreover, the experimental results indicated significantly improved ethylene and propylene yields. For each tonne of ethylene product, the ROC process has the potential to reduce the overall thermal energy demand by 52% when compared with steam cracking. While the conventional naphtha cracking process is estimated to consume 32.5 GJ of energy in order to produce one tonne of ethylene, the ROC only requires a net thermal energy input of 15.5 GJ. The ROC can also provide a reduction of over 50% in CO_2 emissions. Specifically, the upstream section of the ROC process consumes approximately 67% less energy while producing 28% more ethylene and propylene for every kilogram of naphtha feedstock. The absence of the cracking furnaces also results in a considerable reduction in NO_x emissions for the ROC process. Overall, the current study indicates that the novel ROC concept has the potential to be an attractive and environmentally friendly option for ethylene and propylene production from naphtha.

Acknowledgements

This work was supported by the US National Science Foundation (CBET-1604605) and the Kenan Institute for Engineering, Technology and Science at North Carolina State University.

Compliance with ethics guidelines

Vasudev Pralhad Haribal, Yun Chen, Luke Neal, and Fanxing Li declare that they have no conflict of interest or financial conflicts to disclose.

Appendix A. Supplementary data

Supplementary data associated with this article can be found, in the online version, at https://doi.org/10.1016/j.eng.2018.08.001.

References

[1] Moreira JV. Steam cracking: kinetics and feed characterisation [dissertation]. Lisbon: Instituto Superior Técnico; 2015.
[2] Zimmermann H, Walzl R. Ethylene. Ullmann's encyclopedia of industrial chemistry. Weinheim: Wiley-VCH; 2000.
[3] Ren T, Patel M, Blok K. Olefins from conventional and heavy feedstocks: energy use in steam cracking and alternative processes. Energy 2006;31(4):425–51.
[4] Shahrokhi M, Masoumi ME, Sadrameli SM, Towfighi J. Simulation and optimization of a naphtha thermal cracking pilot plant. Iran J Chem Chem Eng 2003;22:27–35.
[5] Masoumi M, Shahrokhi M, Sadrameli M, Towfighi J. Modeling and control of a naphtha thermal cracking pilot plant. Ind Eng Chem Res 2006;45(10):3574–82.
[6] Gärtner CA, van Veen AC, Lercher JA. Oxidative dehydrogenation of ethane: common principles and mechanistic aspects. ChemCatChem 2013;5(11):3196–217.
[7] Cavani F, Ballarini N, Cericola A. Oxidative dehydrogenation of ethane and propane: how far from commercial implementation? Catal Today 2007;127(1):113–31.
[8] Boyadjian C, Lefferts L, Seshan K. Catalytic oxidative cracking of hexane as a route to olefins. Appl Catal Gen 2010;2(372):167–74.
[9] Boyadjian C, Ağıral A, Gardeniers JGE, Lefferts L, Seshan K. Oxidative conversion of hexane to olefins-influence of plasma and catalyst on reaction pathways. Plasma Chem Plasma Process 2011;31(2):291–306.
[10] Boyadjian CA. Oxidative cracking of *n*-hexane: a catalytic pathway to olefins [dissertation]. Enschede: University of Twente; 2010.
[11] Elbadawi AH, Khan MY, Quddus MR, Razzak SA, Hossain MM. Kinetics of oxidative cracking of *n*-hexane to olefins over VO_x/Ce-Al_2O_3 under gas phase oxygen-free environment. AIChE J 2017;63(1):130–8.
[12] Bhasin MM, McCain JH, Vora BV, Imai T, Pujadó PR. Dehydrogenation and oxydehydrogenation of paraffins to olefins. Appl Catal Gen 2001;221(1):397–419.
[13] De Graaf EA, Rothenberg G, Kooyman PJ, Andreini A, Bliek A. $Pt_{0.02}Sn_{0.003}Mg_{0.06}$ on γ-alumina: a stable catalyst for oxidative dehydrogenation of ethane. Appl Catal Gen 2005;278(2):187–94.
[14] Ballarini N, Cavani F, Cericola A, Cortelli C, Ferrari M, Trifirò F, et al. Supported vanadium oxide-based catalysts for the oxidehydrogenation of propane under cyclic conditions. Catal Today 2004;91–92:99–104.
[15] Contractor RM, Bergna HE, Horowitz HS, Blackstone CM, Malone B, Torardi CC, et al. Butane oxidation to maleic anhydride over vanadium phosphate catalysts. Catal Today 1987;1(1):49–58.
[16] Neal LM, Yusuf S, Sofranko JA, Li F. Alkali-doped manganese oxides as redox catalysts for oxidative dehydrogenation of ethane. In: Proceedings of the 250th ACS National Meeting & Exposition; 2015 Aug 16–20; Boston, MA, USA; 2015.
[17] Haribal VP, Neal LM, Li F. Oxidative dehydrogenation of ethane under a cyclic redox scheme—process simulations and analysis. Energy 2017;119:1024–35.
[18] Yusuf S, Neal LM, Li F. Effect of promoters on manganese-containing mixed metal oxides for oxidative dehydrogenation of ethane via a cyclic redox scheme. ACS Catal 2017;7(8):5163–73.
[19] Gao Y, Neal LM, Li F. Li-promoted $La_xSr_{2-x}FeO_{4-\delta}$ core–shell redox catalysts for oxidative dehydrogenation of ethane under a cyclic redox scheme. ACS Catal 2016;6(11):7293–302.
[20] Li F, Neal LM, Zhang J, inventors; North Carolina State University, assignee. Redox catalysts for the oxidative cracking of light hydrocarbons, methods of making, and methods of use thereof. PCT patent WO 2018049389. 2018 Mar 15.
[21] Schefflan R. Teach yourself the basics of aspen plus. Hoboken: American Institute of Chemical Engineers; 2011.
[22] Moulijn JA, van Diepen A, Makkee M. Chemical process technology. 2nd ed. Chichester: John Wiley & Sons Inc.; 2013.
[23] Rochelle GT. Amine scrubbing for CO_2 capture. Science 2009;325(5948):1652–4.
[24] Yan M. Simulation and optimization of an ethylene plant [dissertation]. Lobbock: Texas Tech University; 2000.
[25] Ball M, Basile A, Veziroglu TN. Compendium of hydrogen energy: hydrogen use, safety and the hydrogen economy. Sawston: Woodhead Publishing; 2015.
[26] Hall SM. Rules of thumb for chemical engineers. 5th ed. Oxford: Butterworth-Heinemann; 2012.
[27] Battiston GC, Dalloro L, Tauszik GR. Performance and aging of catalysts for the selective hydrogenation of acetylene: a micropilot-plant study. Appl Catal 1982;2(1):1–17.
[28] Hassan G, Pourkashanian M, Ingham D, Ma L, Newman P, Odedra A. Predictions of CO and NO_x emissions from steam cracking furnaces using GRI2.11 detailed reaction mechanism—a CFD investigation. Comput Chem Eng 2013;58:68–83.